Nano Vision, Vol.3 (2), 76-83 (2013)

Preparation of ZnO Nanoparticles and Its Electrochemical Studies

MAHMUDUR RAHMAN IDRIS and MD. EMRAN QUAYUM

Department of Chemistry,
University of Dhaka, Dhaka, BANGLADESH

(Received on: June 2, 2013)

ABSTRACT

A simple combustion method was followed in the preparation of ZnO nanoparticles. The prepared sample was purified by conventional method (thermal decomposition) in order to use in the environmental detection of pollutants and to apply as nanoelectrodes for monitoring the redox behavior of different redox couples and biomolecules. These particles were characterized by SEM. The prepared ZnO nanocrystals exhibits the hexagonal Wurzite structure. Simple combustion method gives nanoclusters with size ranging from 76-123nm. On the other hand commercial ZnO consisted of particle size of $\leq$ 300nm. The electrochemical behavior of Cu^{2+} , Fe^{3+}/Fe^{2+} redox couple have been studied at Pt electrode, ITO(Indium Tin Oxide) electrode and ZnO modified Pt electrode, ITO electrode. It clearly shows that the value of Diffusion Coefficient(D) and Heterogeneous Charge Transfer Constant(K_f) in Cu^{2+} , Fe^{3+}/Fe^{2+} redox couple increased from bare to modified electrode. Therefore ZnO nanoparticles can be used as biosensors for electrophilic and nucleophilic species(contaminant) present in water.

Keywords: Nanoparticles, Cyclic Voltametry, Electrode, Biosensor.

INTRODUCTION

Water pollution has been a serious threat to the environment. The major sources of pollutants are from manufacturing processing industries, particularly chemical and textile industries in which organic dyes are widely used. Presently, the perilous effects of organic dyes to the environment are aparticular concern. There is a growing

interest in using ZnO as an alternative electrode very recently. Nanostructured porous ZnO film was developed by a simple chemical solution process.

A facile and fast sonochemical route for the fabrication of a resistive-type ZnO gas sensor has been demonstrated. Vertically-aligned ZnO nanorod arrays were grown on a Pt-electrode patterned alumina substrate under ambient conditions. The average diameter and length of the ZnO nanorods were 50 and 500 nm, respectively. Sonochemically grown ZnO nanorod gas sensor was highly sensitive to NO_2 gas with a very low detection limit of 10 ppb at 250 ^oC; further, its response and recovery time were short. Considering the advantageous properties of this sonochemical technique, we believe that it can be used to fabricate high-performance gas sensors.[1]

Nanostructured zinc oxide (nano-ZnO) film has been fabricated onto indium tin oxide (ITO) containing preferred (002) plane and 10 nm crystallite size using sol-gel technique for immobilization of cholesterol oxidase (ChOx)[2]. Electrochemical response of ChOx/nano-ZnO/ITO bioelectrode determined as a function of cholesterol concentration using cyclic voltammetry technique reveals improved detection range (5–400 mg/dl), low detection limit (0.5 mg/dl), fast response time (10 s), sensitivity (0.059 μA/mg dl^{-1} cm^{-2}), and low value (0.98 mg/dl) of Michaelis–Menten constant (K_m). It is shown that nano-ZnO film provides better environment and enhanced electron transfer between ChOx and electrode[3].

Nano-metal oxide coatings. Zinc oxide (ZnO) nanoparticles embedded in polymer matrices like soluble starch are a good example of functional nanostructures with potential for applications such as UV-protection ability in textiles and sunscreens, and antibacterial finishes in medical textiles and inner wears.

Of these, however, it is still a challenge to find a simple fabrication process to prepare ZnO NPs with a large active surface area. In addition, the use in agricultural and environmental aspect requires a simple, cost-effective fabrication process to synthesize ZnO NPs, which can provide a high yield with reasonable purities. Solution-combustion process is simple and cost-effective, expected to provide extremely porous structure of ZnO NPs[4]. With this advantage, the solution-combustion method has been employed to fabricate ZnO NPs, with a mixture of ethanol and ethyleneglycol (V/V = 60/40) as the solvent and zinc acetate as the zinc source. Here ZnO applied as Nanoelectrodes for monitoring the redox behavior of different redox couples and biomolecules. ZnO nanoparticles were also deposited on the Pt and ITO electrodes by electrochemical method. The electrochemical behaviors of different metal ions and metal ligand complexes at bare electrodes and nano ZnO deposired electrodes have been investigated.

RESULT AND DISCUSSION

A spirit lamp containing $Zn(OAc)_2$and an ethanol-ethyleneglycol mixture. (b) Yellow-colored ZnO deposited around the burning lampwick. (c) The yellow-coloredZnO turned white, indicatingthe formation of ZnO NPs. (d) A separated portion of the lampwick with ZnO NPs. (e) ZnO NPs peeled off, dispersed in water, and dried at 500°C.

The resultant white product was repeatedly peeled off and dispersed in distilled water to remove the impurity. The prepared sample was taken into a crucibal and the crucibal was put into Muffle furnace for heating. The sample was heated about six hours at a temperature 500^{o} C. After heating white sample was collected and finally preserved in an airtight desiccator. Scanning electron microscope (SEM) images were taken by a Scanning Electrode Micriscope (Hitachi S-3400N, Japan), from BCSIR.

The scale bars in the micrographs represent 2 µm SEM image of the microstructure ZnO NPs prepared by the combustion method is depicted in Figure 2, showing that most particles exhibited an ellipsoidal shape. Some small particles with a rounded shape and few large particles were also seen. The bigger-sized particles ought to be attributed to the aggregation or overlapping of small particles. The particle size measured from the SEM micrographs was in the range of 76 to 120 nm for short-length axes and 100 to 400 nm for long-length axes. Thus, the topological images suggested that particle sizes were not well defined; it might be resultant of uncontrolled ambient conditions.

Fig.3 CV of 2.00 mM Cu^{2+} ion on Modified Pt electrode at (a) 0.05 Vs^{-1},(b) 0.075 Vs^{-1} and,(c) 0.10 Vs^{-1} scan rate. CV of 2.00 mM Cu^{2+} ion at different scan rates on modified Pt electrode is presented in Fig 3 The potential was stepped from +0.80 V to a vertex potential of -0.80 V and finally the potential was reversed back to +0.80 V. The first cathodic peak was observed at +0.106 V and the second cathodic peak appeared at -0.050 V. The corresponding anodic peak was observed at +0.139V and -0.060V respectively. Both cathodic and anodic peak current increases with increasing scan rate but peak potential remains almost constant.

Fig. 4 CV of 2.00 mM Cu^{2+} ion on Pt electrode at (a) 0.05 Vs^{-1},(b) 0.075 Vs^{-1} and,(c) 0.10 Vs^{-1} scan rate.It shows the CV of 2.00 mM Cu^{2+} ion at different scan rates on Pt electrode. The potential was stepped from +0.80 V to a vertex potential of -0.80 V and finally the potential was reversed back to +0.80 V. The first cathodic peak was observed at +0.099 V and the second cathodic peak appeared at -0.200 V. The corresponding anodic peak was observed at +0.150 V and -0.063 V respectively. Both cathodic and anodic peak current increases with increasing scan rate but peak potential remains almost constant.

Fig. 5 CV of 2.00 mM Cu^{2+} ion at (b) Pt electrode (a) ZnO modified Pt electrode at scan rate 100 mVs^{-1}. Here the CV of Cu^{2+} shows the first cathodic peak for Pt electrode and modified Pt electrodes are almost at same potential**.** The potential of second cathodic peak shifted towards positive potential for modified Pt electrode.Both cathodic and anodic peak current increases significantly in the case of modified Pt electrode.

(a) Charge transfer rate constant for reversible system, $K_{f(rev).}$is 1.658 x 10^{-3} cm/s and for quasi-reversible system $K_{f(rev).}$ is 1.1174 x 10^{-3} cm/s at modified Pt electrode.

(b) Charge transfer rate constant for reversible system, $K_{f(rev).}$is 2.156 x 10^{-3} cm/s and for quasi-reversible system $K_{f(rev).}$ is 1.295 x 10^{-3} cm/s at Pt electrode.

Fig. 6 CV of 0.40 mM $K_3Fe(CN)_6$ solution at (a) 0.015 mVs^{-1} (b) 0.020 mVs^{-1} (c) 0.025 mVs^{-1} S.R

Fig. 6 is the CV of 0.40 mM $K_3Fe(CN)_6$ solution at different scan rates on modified ITO electrode. The potential was stepped from +0.650 V to a vertex potential of -0.150 V and finally the potential was reversed back to +0.650 V. The cathodic peak was observed at +0.162 V. The corresponding anodic peak was observed at +0.245 V. Both cathodic and anodic peak current increases with increasing scan rate and the peak potential remain almost constant.

Fig. 7 CV of 0.40 mM $K_3Fe(CN)_6$ solution at (a) 0.015 mVs^{-1} (b) 0.020 mVs^{-1} (c) 0.025 mVs^{-1} S.R

Fig. 7 shows the CV of 0.40 mM $K_3Fe(CN)_6$ solution at different scan rates on ITO electrode. The potential was stepped from +0.650 V to a vertex potential of -0.150 V and finally the potential was reversed back to +0.650 V. The cathodic peak was observed at +0.160V. The corresponding anodic peak was observed at +0.233 V. Both cathodic and anodic peak current increases with increasing scan rate and potential remain almost constant.

Fig. 8 CV of $K_3[Fe(CN)_6]$ solution at (b) ITO electrode and (a) modified ITO electrode at S.R 25 mVs^{-1}. In Fig 8 CV of 0.40 mM $K_3[Fe(CN)_6]$ solution at (a) ZnO modified ITO electrode (b) ITO electrode at scan rate 25 mVs^{-1} Here the CV of $K_3[Fe(CN)_6]$ solutions show that both the cathodic and anodic peak potential are almost at the same position for ITO electrode and modified ITO electrode. But the current increases significantly in the case of ZnO modified ITO electrode.

(a) Charge transfer rate constant for reversible system, K_f(rev) is 4.834 x 10^{-4} cm/s, at modified ITO electrode.

Charge transfer rate constant for reversible system, K_f(rev) is 1.857 x 10^{-4} cm/s at ITO electrode.

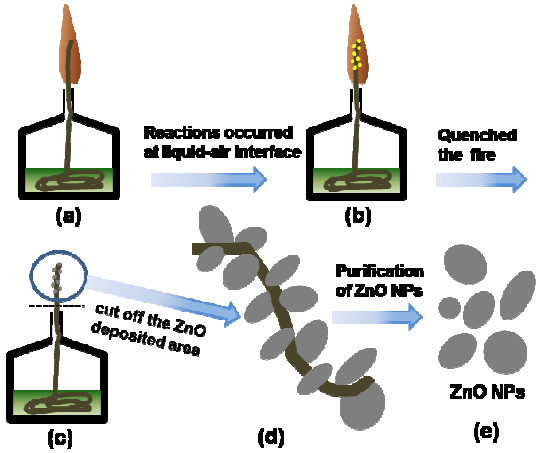

Figure 1 The fabrication process of ZnO NPs by a simple combustion method.

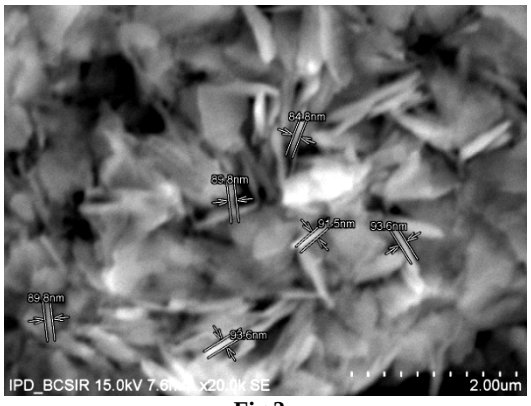

Fig.2a

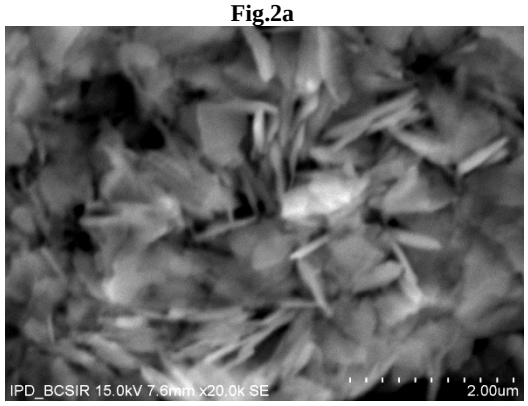

Fig.2b

Figure 2 SEM micrographs of the prepared ZnO NP .

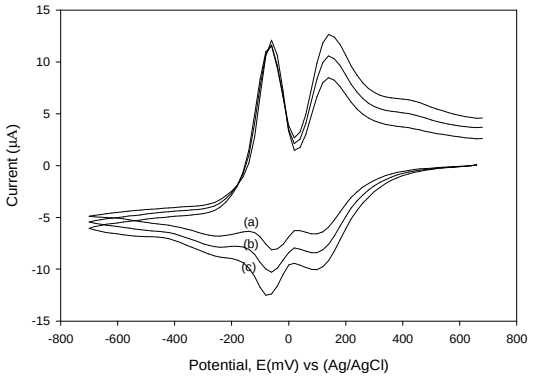

Figure 3 Electrochemical behaviour of Cu^{2+} on Pt electrode at different scan rates

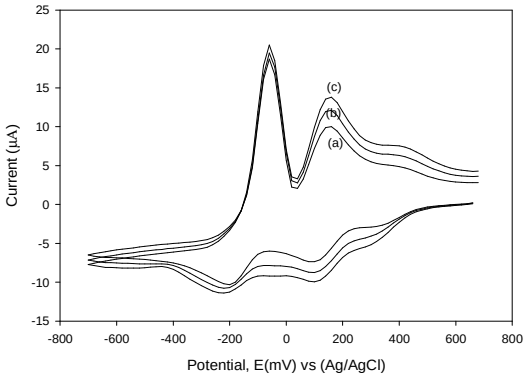

Figure 4 Electrochemical behaviour of Cu^{2+} on ZnO modified Pt electrode for different scan rates

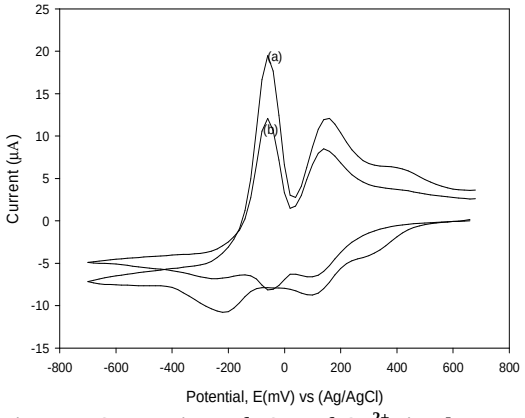

Figure 5 Comparison of CV of Cu^{2+} ion between Pt electrode and ZnO modified Pt electrode

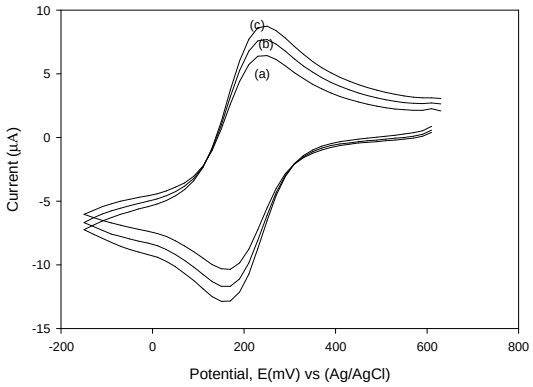

Figure 6 Electrochemical behaviour of $K_3Fe(CN)_6$ on ITO electrode for different scan rates

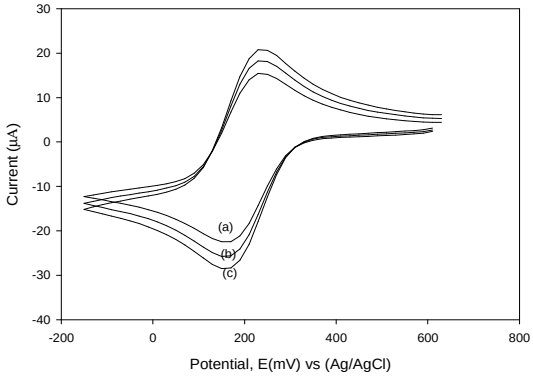

Figure 7 Electrochemical behaviour of $K_3Fe(CN)_6$ on ZnO mpdified ITO electrode for different scan rates

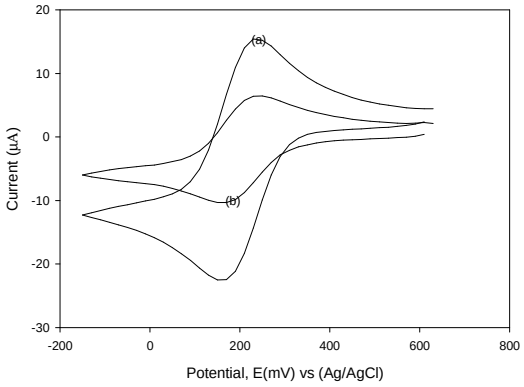

Figure 8 Comparison of CV of $K_3[Fe(CN)_6]$ solution between ITO electrode and ZnO modified ITO electrode

METHODS

This study was accomplished in the Department of Chemistry, University of Dhaka, Babgladesh. All chemicals were purchased from the market and used as received. In this study, $Zn(CH_3COO)_2.2H_2O$ (0.03 mol) was dissolved in 100 mL of a mixed-solvent system of ethanol-ethyleneglycol in a volume ratio of 60/40. A portion of this mixture was transferred to a spirit lamp including an absorbent cotton lampwick. The spirit lamp was ignited, and after a certain time, a yellowish-colored substance formed around the surface of the ignited lampwick. When the lampwick was quenched, the yellow-colored substance turned white. A schematic diagram of the fabrication process is shown in Figure 1. It has been reported that the interaction between zinc acetate and alcohol under solvothermal conditions follows the esterification reaction, yielding ZnO, ester, and water[4-6], according to the following reaction:

Table 1 : Comparisons of diffusion co- efficient of Cu^{2+} in Pt, ITO electrodes and modified Pt, modified ITO electrodes

Diffusion co-efficient D x 10^{-6} (cm^2sec^{-1})	Cu^{2+} at Pt Electrode (2.00 mM)	Cu^{2+} at ZnO modified Pt electrode (2.00mM)	Cu^{2+} at ITO electrode (0.4mM)	Cu^{2+} at ZnO modified ITO electrode (0.4mM)
Reversible system	7.07	9.43	95.46	78.05
Quasi Reversible system	10.23	13.57	30.99	91.77

Table 2 : Comparisons of diffusion co- efficient of $K_3Fe(CN)_6$ in Pt, ITO electrodes and modified Pt, modified ITO electrodes:

Diffusion co-efficient D x 10^{-6} (cm^2sec^{-1})	$K_3Fe(CN)_6$ at Pt Electrode (1.00 mM)	$K_3Fe(CN)_6$ at Modified Pt Electrode (1.00 mM)	$K_3Fe(CN)_6$ at ITO Electrode (0.40 mM)	$K_3Fe(CN)_6$ at modified ITO Electrode (0.40 mM)
Reversible system	0.65	0.76	3.25	5.56

$$Zn\left(CH_3COO\right)_2 + 2R-OH \rightarrow ZnO + 2CH_3-CO-R + H_2O$$

Cyclic voltammetry is one of the most versatile electro analytical techniques for the study of redox behavior of electroactive species. The principles of CV have been discussed by Kissinger and Heineman[7]. Organic chemists have applied the techniques to study biosynthetic reaction pathways[8] and to study the electro chemically generated free radicals[9].

The conventional three electrode cell in which ZnO were prepared was maintained at 40^o C in a water bath. The working electrode was a commercial ITO glass (30 x 66.66 x 6 mm, R(s) < 10 ohm).

An aqueous solution of 0.1M $Zn(NO_3)_2$ mixed with 0.1 M KCl was used and deposition was carried out for one hour. ZnO nanoparticles were electrodeposited on ITO electrode(area 3.2 cm^2) at -1.1 V vs Ag/AgCl reference electrode and a Pt electrode(area 0.03cm^2) was used as counter electrode. After deposition the resulting nenodeposits were thoroughly rinsed with water and dried under a nitrogen atmosphere. ZnO nanoparticles were electrodeposited on the surface of Pt electrode by applying fixed potential (-0.8 V for initial delay 120 s) from a zinc acetate solution with 40^0 C.

CONCLUSION

A novel, feasible, and cost-effective process of fabricating ZnO NPs was successfully demonstrated, which would be a very promising method for synthesizing other semiconductor NPs. The chemical reactions occurred at the solvent-air interface, yielding ZnO NPs via esterification of alcohol. The NPs exhibited a nonuniform size and shape which might be due to the uncontrolled growth; however, controlled processing parameters might produce a uniform size and shape of the particles. The electrochemical behaviors of Cu^{2+} ion and Fe(III)/Fe(II) redox couple have been studied at Pt electrode, ITO electrode and modified Pt electrode and modified ITO electrode. The Cu^{2+} ion system follows a two step reduction process in the cathodic region of the cyclic voltammogram. The corresponding anodic peaks for Cu^{2+} ion system represent two step oxidation processes. It is clear from the CV that the 1st system follows a reversible and 2nd system follows a quasi-reversible charge transfer process in bare Pt electrode and modified Pt electrode. The diffusion co-efficient (D) and heterogeneous charge transfer rate constant (kf) increases from bare to modified Pt electrode. Again in the reversible Fe(III)/Fe(II) redox couple in $K_3Fe(CN)_6$, the D and K_f values increases from bare to Modified ITO electrode. Therefore ZnO nanoparticles can be used as sensors for electrophillicand nucleophillic species present in the environment. Further investigations can be carried out in this field.

ACKNOWLEDGMENTS

The authors thank the Bangladesh Council of Scientific and Industrial Research, Dhaka, Bangladesh for the SEM images.

REFERENCES

1. Jiej S, Wang G Z, Wang Q T, Chen Y M. Han X H. Wang P and Hou G, *J. Phys. Chem* B 108 11976, (1991).
2. Wing. Jackie. Nanostructured Materials. Newyork: Academic Press, (2001).
3. Analytical Electrochemistry by Joseph Wang/page32.
4. Ni, Y., Cao, X., Wu, G., Hu, G., Yang, Z., Wei, X.: Preparation, characterization and property study of zinc oxide nanoparticles via a simple solution-combusting method. *Nanotechnology* 18, 155603–155608 (2007).
5. Yiamsawas, D., Boonpavanitchakul, K., Kangwansupamonkon, W.: Preparation of ZnO nanostructures by solvothermal method. *J. Micros. Soc. Thailand* 23(1), 75–78 (2009).
6. Bell, N. S. : Solvothermal routes for synthesis of zinc oxide nanorods. *Symp Pros. Mater Res. Soc.* 878E, Y2.6.1–Y2.6.11 (2005)

7. I. Poilios; I Tsachpinis; *J. Chem. Technol. Biotechnol*. 74(4), 349-457 (1999).
8. Liu, Guangmin; Wu, Taixing; Zhao, Jincai; Hidaka, Hisao; Surpone, Nick; *Environ. Sci. Technol*. 33(2), 2081-2087 (1999).
9. F. Kiriakidou; d. I. Kondarides; X. E. Verikyous; *Catal. Today*, 54(1), 119-130 (1999).